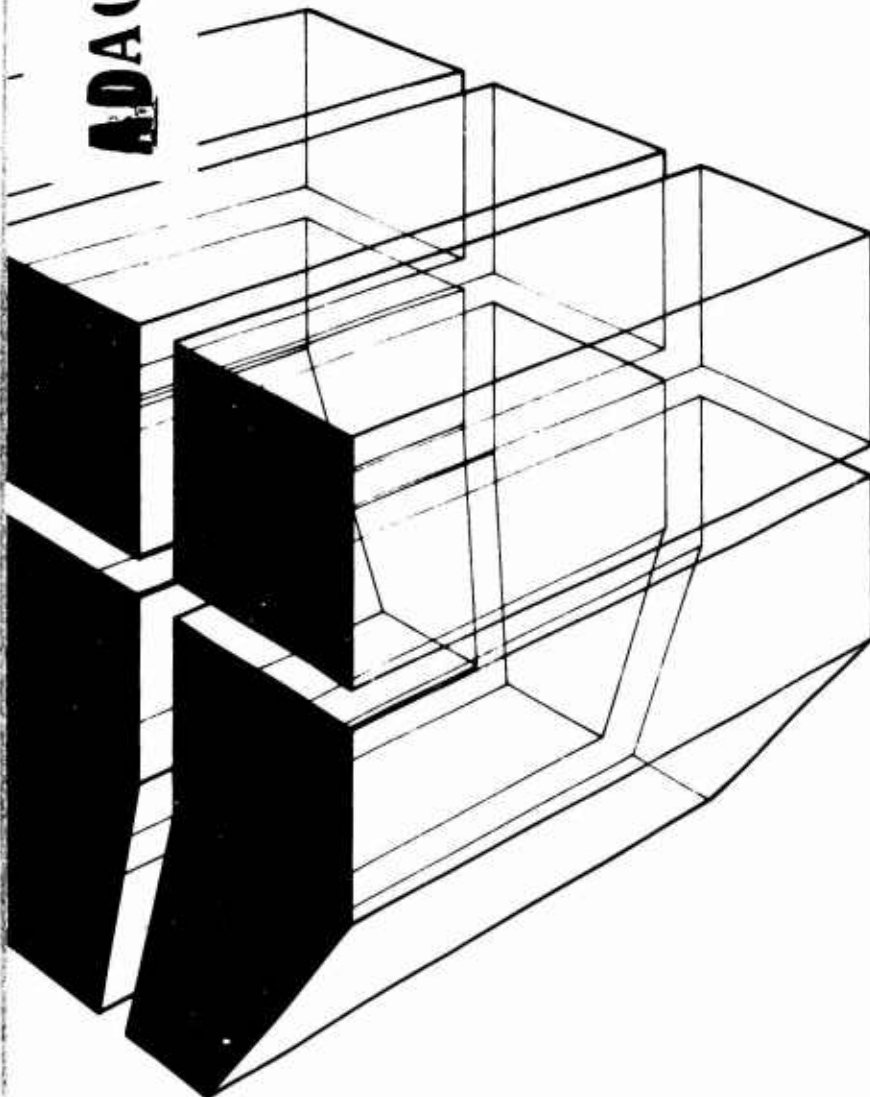


construction  
engineering  
research  
laboratory

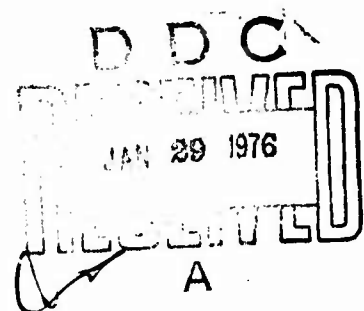
DD  
TECHNICAL REPORT M-171  
November 1975  
Hardness Assurance Assessment

RFI SHIELDING EFFECTIVENESS OF STEEL SHEETS WITH  
PARTLY WELDED SEAMS

ADAU19931



(12)  
by  
E. M. Honig, Jr.



Approved for public release ; distribution unlimited.

The contents of this report are not to be used for advertising, publication, or promotional purposes. Citation of trade names does not constitute an official indorsement or approval of the use of such commercial products. The findings of this report are not to be construed as an official Department of the Army position, unless so designated by other authorized documents.

**DESTROY THIS REPORT WHEN IT IS NO LONGER NEEDED  
DO NOT RETURN IT TO THE ORIGINATOR**

UNCLASSIFIED

SECURITY CLASSIFICATION OF THIS PAGE (When Data Entered)

REPORT DOCUMENTATION PAGE		READ INSTRUCTIONS BEFORE COMPLETING FORM
1. REPORT NUMBER 14 CERL-TR-M-171	2. GOVT ACCESSION NO.	3. RECIPIENT'S CATALOG NUMBER
4. TITLE (and Subtitle) 6 REI SHIELDING EFFECTIVENESS OF STEEL SHEETS WITH PARTLY WELDED SEAMS.		5. TYPE OF REPORT & PERIOD COVERED 9 FINAL rept.
7. AUTHOR(s) 10 E. M. Honig, Jr.		6. PERFORMING ORG. REPORT NUMBER
9. PERFORMING ORGANIZATION NAME AND ADDRESS CONSTRUCTION ENGINEERING RESEARCH LABORATORY P.O. Box 4005 Champaign, IL 61820		8. CONTRACT OR GRANT NUMBER(s) 12 22 p.
10. PROGRAM ELEMENT, PROJECT, TASK AREA & WORK UNIT NUMBERS 16 DA-4A162118A880/11-003		11. REPORT DATE 11 November 1975
11. CONTROLLING OFFICE NAME AND ADDRESS 17 4-A-162118-A-05011		12. NUMBER OF PAGES 27
14. MONITORING AGENCY NAME & ADDRESS (if different from Controlling Office)		15. SECURITY CLASS. (of this report) Unclassified
		15a. DECLASSIFICATION/DOWNGRADING SCHEDULE
16. DISTRIBUTION STATEMENT (of this Report) Approved for public release; distribution unlimited.		
17. DISTRIBUTION STATEMENT (of the abstract entered in Block 20, if different from Report)		
18. SUPPLEMENTARY NOTES Copies are obtainable from National Technical Information Service Springfield, VA 22151		
19. KEY WORDS (Continue on reverse side if necessary and identify by block number) shielding effectiveness weld defects electromagnetic shielded enclosures porosity		
20. ABSTRACT (Continue on reverse side if necessary and identify by block number) This report presents the results of an investigation to determine the effect of six forms of incomplete welds containing slots and holes on the shielding effectiveness of shielded enclosures. The test specimens were butted plates and slotted plates (with and without tacked backing strips), wide-slot plates, and drilled plates. The plates were subjected to radio frequency interference (RFI) radiation from nominally 10 kHz to 10 GHz in frequency. Shielding effectiveness as a function of flaw size was determined for each defect class. Three critical, or transition, flaw sizes were determined for the three minimum specified shielding levels for each class of defect. Since through-thickness slots and holes → OVER		

UNCLASSIFIED

SECURITY CLASSIFICATION OF THIS PAGE(When Data Entered)

Block 20 continued.

are limiting, or worst, cases of cracks and porosity respectively, the critical flaw sizes determine the sizes of the cracks and porosity in welds that are not cost-effective to repair.

Results showed that weld seams having unwelded, but tightly butted, lengths up to 4½ in. (11.43 cm) afford at least 60 dB shielding effectiveness at all test frequencies. Slots of finite width seriously compromise shielding by acting as resonant radiators. Backing strips tacked (without burn-through) over welded seams have minor effect on shielding effectiveness. Holes up to 0.3 in. (0.762 cm) can be tolerated at all test frequencies since at least 60 dB shielding effectiveness is maintained.

X

LA

UNCLASSIFIED

SECURITY CLASSIFICATION OF THIS PAGE(When Data Entered)

## FOREWORD

This investigation was performed for the Directorate of Military Construction, Office of the Chief of Engineers (OCE), under Project 4A162118A880, "Nuclear Construction and Engineering"; Task 11, "Advanced BMD Facilities, Engineering Design Criteria"; Work Unit 003, "Hardness Assurance Assessment." The OCE Technical Monitor was Mr. D. S. Reynolds.

This investigation was performed by the Metallurgy Branch, Materials Systems and Science Division (MS), U.S. Army Construction Engineering Research Laboratory (CERL). CERL personnel directly involved in the study were Mr. F. H. Kisters and Dr. E. M. Honig, Jr. of the MS Metallurgy Branch; Messrs. R. McCormack, P. Nielson, J. Simon, and M. J. Pollock of the Electro-Mechanical Branch, Facilities Engineering and Construction Division; and Mr. H. Stringfellow of the Support Office Technical Services Branch.

Dr. R. Quattrone is Chief of the Metallurgy Branch and Dr. W. E. Fisher is Acting Chief of MS. COL M. D. Remus is Commander and Director of CERL, and Dr. L. R. Shaffer is Deputy Director.

## CONTENTS

DD FORM 1473	1
FOREWORD	3
LIST OF TABLES AND FIGURES	5
1 INTRODUCTION . . . . .	7
Background	
Objective	
Approach	
2 PROCEDURE. . . . .	7
Specimen Fabrication	
Conduct of Tests	
3 RESULTS AND ANALYSIS . . . . .	10
4 CONCLUSIONS AND RECOMMENDATIONS . . . . .	14
Conclusions	
Recommendations	
REFERENCES	15
FIGURES	16
DISTRIBUTION	

## TABLES

Number	Page
1 Procedural Data for Butted Plates	8
2 Procedural Data for Slotted Plates	8
3 Procedural Data for Wide-Slot Plates	9
4 Procedural Data for Backing-Strip Plates	9
5 Procedural Data for Slotted Backing-Strip Plates	10
6 Procedural Data for Drilled Plates	10
7 Equipment Used for Shielding Effectiveness Measurements	11
8 Transition Flaw Sizes for Various Test Geometries	13

## FIGURES

1 Butted Plate With 12.1-in. Slot Length	16
2 Slotted Plate With Slot 9.44 in. Long and 1/16 in. Wide—Shielded Enclosure Side	17
3 Wide-Slot Plate With Slot 3.54 in. Long and 1/2 in. Wide—Shielded Enclosure Side	17
4 Backing-Strip Plate With 3.54-in. Long Slot	18
5 Drilled Plates—Shielded Enclosure Sides	19
6 Shielded Enclosure With Cover Plate Over Test Panel and Door Into One of Two Compartments	19
7 Transmitter Side of Test Panel Bolted Over Aperture of Shielded Enclosure	20
8 View of Same Panel From Within Shielded Enclosure	20
9 Receiving Antenna Positioned Before Test Panel	21
10 Shielding Effectiveness vs Frequency	21
11 Shielding Effectiveness vs Slot Length for Butted Plates—10 kHz to 1 MHz	22
12 Shielding Effectiveness vs Slot Length for Butted Plates—30 MHz to 10 GHz	22
13 Shielding Effectiveness vs Slot Length for Slotted Plates—10 kHz to 1 MHz	23
14 Shielding Effectiveness vs Slot Length for Slotted Plates—30 MHz to 10 GHz	23

## FIGURES (Cont.)

Number		Page
15	Shielding Effectiveness vs Slot Length for Wide-Slot Plates 10 kHz to 1 MHz	24
16	Shielding Effectiveness vs Slot Length for Wide-Slot Plates 30 MHz to 9.09 GHz	24
17	Shielding Effectiveness vs Slot Length for Backing-Strip Plates 10 kHz to 1 MHz	25
18	Shielding Effectiveness vs Slot Length for Backing-Strip Plates 30 MHz to 9.09 GHz	25
19	Shielding Effectiveness vs Slot Length for Slotted Backing-Strip Plates 10 kHz to 1 MHz	26
20	Shielding Effectiveness vs Slot Length for Slotted Backing-Strip Plates - 30 MHz to 9.09 GHz	26
21	Shielding Effectiveness vs Hole Diameter for Drilled Plates -10 kHz to 1 MHz	27
22	Shielding Effectiveness vs Hole Diameter for Drilled Plates 30 MHz to 10 GHz	27



# RFI SHIELDING EFFECTIVENESS OF STEEL SHEETS WITH PARTLY WELDED SEAMS

## 1 INTRODUCTION

### Background

Current specifications, largely unsupported by experimental data, require weld seams in electromagnetically shielded facilities to be radiographically defect-free. These specifications have necessitated spending \$1,000,000 for inspection and weld rework at SAFE-GUARD missile sites. In a study of the effect of weld defects on the shielding effectiveness of shielded enclosures containing welded seams, Carlson found that weld seams having weld defects under a critical size could provide adequate shielding effectiveness, and that repair of such seams was an unnecessary expense.<sup>1</sup> He suggested that the effect of crack (or slot) width and length on shielding effectiveness be evaluated in a future study that would determine critical sizes for classes of defects and would investigate circumstances in which a flaw might act as a resonant antenna.

### Objective

The objectives of this study were twofold: to determine the effect of certain large welding defects on the shielding effectiveness of steel plates; and to determine the critical size below which cracks and porosity in welds do not degrade shielding effectiveness below specifications and are thus uneconomical to repair.

### Approach

Welded steel panels containing through-thickness slots and holes of varying sizes in welds were tested for shielding effectiveness in a high-quality shielded enclosure. These defects were considered as limiting, or worst, cases of cracks and porosity in welds. The tests for each panel covered a frequency range from 10 kHz to 9.5 GHz. Degradation of shielding effectiveness as a function of disturbance size and geometry was noted. Applying specifications for minimum shielding effectiveness as a function of frequency to these data produced critical sizes for each of the aperture geometries.

The slot lengths chosen were multiples of the quarter-wavelengths of the higher radio frequencies transmitted through the test panels into the shielded enclosure.

<sup>1</sup>K. W. Carlson, *The Effect of Weld Defects on RFI Shielding Effectiveness*, Technical Report M-43/AD773716 (Construction Engineering Research Laboratory [CERL], January 1974).

If incident radiation has wavelength  $\lambda$ , and slot length is  $\lambda/2$ , the slot can act as a resonant cavity of the first order. An Nth order cavity results from slots of length  $N\lambda/2$ . It was hypothesized that anti-resonance might result from a slot of length  $\lambda/4$ . Such a condition, if obtainable, could produce a sharp rise in shielding effectiveness as a function of slot length, contrasting with the sharp drop produced by resonance. To test the resonance and anti-resonance concepts, some slot lengths were made equal to the resonant wavelengths (even multiples of  $\lambda/2$ ), while others were made equal to odd multiples of  $\lambda/4$ . The resonant slots can also be considered as waveguides for the fundamental transverse-electric (TE) rectangular waveguide mode,  $TE_{01}$ . The null index indicates a wave propagation through a slotlike waveguide.

Through-plate holes in resonant sizes were also desired. Since determination of resonant size for holes is mathematically more sophisticated than for slots, the holes were likened to circular waveguides, and certain hole diameters were chosen for resonance in low-order transverse-electric (TE) and transverse-magnetic (TM) circular waveguide modes.

## 2 PROCEDURE

### Specimen Fabrication

Each specimen was composed of two 11-gage (approximately 1/8 in. or 0.32 cm thick), 8 in. x 24 in. (20.32 cm x 60.96 cm), low-carbon steel panels butted together and gas-metal arc welded. Slot flaws were made by leaving an unwelded seam of the desired length in the central portion of the weld line (Figure 1). Contraction of the adjacent weld metal during cooling kept the contiguous unwelded edges of each specimen tightly butted. Welds were made in a single pass from the side of the panel that was intended to face the shielded enclosure. Full penetration welds were made, and excess weld metal was ground off. Each weld was radiographed to insure that no effective flaws except the implanted one existed. The side of the panel containing the weld crown was then flame-sprayed with tin to a thickness of about 0.01 in. (0.03 cm). This provided a conducting interface between the panel and the shielded enclosure cover plate for effective attenuation of the Radio Frequency Interference (RFI) signal received in the enclosure from the external source.

The first test series, butted plates (Figure 1), consisted of varying lengths of unwelded seam (Table 1).

**Table 1**  
Procedural Data for Butted Plates  
(Test Series 1)

Specimen Number	Test Order	Slot Length, in. (cm)	Calculated Resonant Frequency (TE <sub>01</sub> Rectangular Mode)
1	11	0.15 ( 0.38)	
2	5	0.31 ( 0.79)	10 GHz*
3	1	0.59 ( 1.50)	10 GHz
4	10	1.18 ( 3.00)	10 GHz**
5	4	2.07 ( 5.26)	
6	3	2.36 ( 5.99)	2.5 GHz
7	13	2.66 ( 6.76)	
8	8	3.24 ( 8.23)	
9	9	3.54 ( 8.99)	
10	6	4.72 (11.99)	2.5 GHz**
11	14	9.44 (23.98)	
12	2	11.51 (29.24)	
13	7	11.80 (29.97)	500 MHz
14	12	12.10 (30.73)	

\*Anti-resonance

\*\*Second-order resonance

To insure that no sprayed tin lay in the slots, concentrated HCl was dripped onto each slot. Since the reaction of tin and HCl creates H<sub>2</sub> gas and a salt of tin and chlorine, the treatment was applied until no evolution of H<sub>2</sub> gas was noted. Seepage of HCl throughout each slot was noted.

The second test series, slotted plates (Table 2), used the plates from the first series with 1/16-in. (0.16 cm) wide slots (Figure 2) milled to the same length as the butted slot length tested in the first series. The third test series, wide-slot plates (Table 3), used the same plates with the three smallest slots widened to 3/16-in. (0.48 cm) (to keep the slot axis horizontal) and the rest to 1/2-in. (1.27 cm) (Figure 3).

The fourth test series, backing-strip plates (Table 4), was fabricated similarly to the first series, with the addition of backing strips. The strips were 2 in. x 13 in. (5.08 cm x 33.02 cm) and were tack-welded to the

**Table 2**  
Procedural Data for Slotted Plates (Test Series 2—Slots  
1/16 in. or 0.16 cm Wide)

Specimen Number	Test Order	Slot Length, in. (cm)	Calculated Resonant Frequency (TE <sub>01</sub> Rectangular Mode)
1	6	0.165 ( 0.419)	
2	4	0.345 ( 0.876)	9.09 GHz*
3	10	0.645 ( 1.638)	9.09 GHz
4	1	1.300 ( 3.302)	2.27 GHz; * 9.09 GHz**
5	8	2.225 ( 5.652)	
6	7	2.595 ( 6.591)	2.27 GHz
7	9	2.915 ( 7.404)	
8	3	3.545 ( 9.004)	
9	5	3.885 ( 9.868)	
10	2	5.170 (13.132)	2.27 GHz; ** 568 MHz*
11	13	10.405 (26.429)	568 MHz
12	11	11.665 (29.629)	
13	12	12.020 (30.531)	

\*Anti-resonance

\*\*Second-order resonance

panels symmetrically about the weld flaw, on the side containing the weld root (Figure 4). The butted panel weld did not penetrate into the strip, thus providing a "worst case" configuration. Since the strip was short enough to fit inside the aperture of the shielded enclosure cover plate to which the specimen plate was bolted during testing, the backing strip was not sandwiched between the test panels and the cover plate. The slots were covered with aluminum adhesive tape prior to flame spraying, to prevent tin from entering the slots.

The fifth test series, slotted backing-strip plates (Table 5), used the plates of the fourth series with 1/16-in. (0.16 cm) wide slots milled as in the second test series. Only the welded plates were slotted; the backing strips were not.

The sixth test series, drilled plates (Table 6), consisted of single holes drilled through otherwise perfect welds (Figure 5) after flame spraying.

**Table 3**  
**Procedural Data for Wide-Slot Plates**  
**(Test Series 3)**

Specimen Number	Test Order	Slot Length, in. (cm)	Slot Width, in. (cm)	Calculated Resonant Frequency (TE <sub>01</sub> Rectangular Mode)
1	11	0.165 (0.419)	3/16 (0.48)	
2	7	0.345 (0.876)	3/16 (0.48)	9.09 GHz*
3	12	0.645 (1.638)	3/16 (0.48)	9.09 GHz
4	5	1.300 (3.302)	1/2 (1.27)	2.27 GHz; * 9.09 GHz**
5	10	2.225 (5.652)	1/2 (1.27)	
6	8	2.595 (6.591)	1/2 (1.27)	2.27 GHz
7	1	2.915 (7.404)	1/2 (1.27)	
8	2	3.545 (9.004)	1/2 (1.27)	
9	6	3.885 (9.868)	1/2 (1.27)	
10	3	5.170 (13.132)	1/2 (1.27)	2.27 GHz; ** 568 MHz*
11	9	10.405 (26.429)	1/2 (1.27)	568 MHz
12	4	11.665 (29.629)	1/2 (1.27)	
13	13	12.020 (30.531)	1/2 (1.27)	

\*Anti-resonance

\*\*Second-order resonance

#### Conduct of Tests

Each test panel was bolted over an aperture in the shielded enclosure (Figure 6), with RFI gasket material sandwiched between the panel perimeter and the enclosure. Figure 7 shows the transmitter side of a slotted plate bolted to the shielded enclosure cover plate; Figure 8 shows the enclosure side of the same panel. Hardened steel bolts were used to compress the test plate and RFI gasket to the cover plate. The bolts were torqued to over 50 ft-lb (67.8 Nm) until no RF leakage through the gasket could be detected by an RF "sniffer," or leak detector.

After bolting, the panels were illuminated by electromagnetic waves of eight different frequencies in sequence. The tests were made in accordance with Military Standard 285<sup>2</sup> and Institute of Electric and Electronic

<sup>2</sup>Method of Attenuation Measurements for Enclosures, Electromagnetic Shielding, for Electronic Test Purposes, MIL-STD-285 (Department of Defense, June 1956).

**Table 4**  
**Procedural Data for Backing-Strip Plates**  
**(Test Series 4)**

Specimen Number	Test Order	Slot Length, in. (cm)	Calculated Resonant Frequency (TE <sub>01</sub> Rectangular Mode)
1	10	0.15 ( 0.38)	
2	9	0.31 ( 0.79)	10 GHz*
3	7	0.59 ( 1.50)	10 GHz
4	2	1.18 ( 3.00)	10 GHz**
5	1	2.07 ( 5.26)	
6	5	2.36 ( 5.99)	2.5 GHz
7	8	2.66 ( 6.76)	
8	13	3.24 ( 8.23)	
9	4	3.54 ( 8.99)	
10	12	4.72 (11.99)	2.5 GHz**
11	6	9.44 (23.98)	
12	11	11.51 (29.24)	
13	3	11.80 (29.97)	500 MHz

\*Anti-resonance

\*\*Second-order resonance

Engineers Standard 299<sup>3</sup>; the attenuated signal received in the shielded enclosure was measured in decibels with respect to free space (uncovered aperture in the enclosure). The electric field vector was perpendicular to the slot axis of slotted test panels. Details of the test arrangement and equipment are presented in the previous study.<sup>4</sup> Table 7 lists the test equipment used.

A shielded septum divided the enclosure into two compartments, each roughly 10 ft (3.04 m) cubed. One compartment supported the test panel and contained the RF receiving antenna (Figure 9). The antenna cable passed through the septum to the receiver in the other compartment. Testing personnel monitored

<sup>3</sup>Measurement of Shielding Effectiveness of High Performance Shielding Enclosures, IEEE Standard 299 (Institute of Electrical and Electronic Engineers, 1969).

<sup>4</sup>K. W. Carlson, The Effect of Weld Defects on RFI Shielding Effectiveness, Technical Report M43/AD773716 (CFRL, January 1974).

**Table 5**  
Procedural Data for Slotted Backing-Strip Plates  
(Test Series 5—Slots 1/16-in or .16 cm Wide)

Specimen Number	Test Order	Slot Length, in. (cm)	Calculated Resonant Frequency (TE <sub>01</sub> Rectangular Mode)
1	9	0.15 ( 0.38)	
2	6	0.31 ( 0.79)	10 GHz*
3	5	0.59 ( 1.50)	10 GHz
4	2	1.18 ( 3.00)	10 GHz**
5	10	2.07 ( 5.26)	
6	7	2.36 ( 5.99)	2.5 GHz
7	8	2.66 ( 6.76)	
8	11	3.24 ( 8.23)	
9	4	3.54 ( 8.99)	
10	13	4.72 (11.99)	2.5 GHz**
11	12	9.44 (23.98)	
12	1	11.51 (29.24)	
13	3	11.80 (29.97)	500 MHz

\*Anti-resonance  
\*\*Second-order resonance

the signals received in the second compartment, which was accessed by a shielded sliding door with a pneumatic shielding gasket.

Experience over a number of projects has shown that a strong resonance in the first compartment of the shielded enclosure exists in the vicinity of 500 MHz. Considering fields in a closed rectangular cavity does not explain this resonance. That theory predicts the first normal frequency, or (110) mode, to be 10 MHz for a 10-ft (3.04 m) cubed room.

The three highest frequencies reported in the previous study<sup>5</sup> were 500 MHz, 2.5 GHz, and 10 GHz. However, 2.5 GHz is the top of the Maxson oscillator's range, and the Narda oscillator is calibrated to only 9.8 GHz (Table 7). Thus the signal at 2.5 GHz was shifted

<sup>5</sup>K. W. Carlson, *The Effect of Weld Defects on RFI Shielding Effectiveness*, Technical Report M-43/AD773716 (CERL, January 1974).

**Table 6**  
Procedural Data for Drilled Plates  
(Test Series 6)

Specimen Number	Test Order	Hole Diameter, in. (cm)	Calculated Circular Mode Resonant at 9.09 GHz
1	1	1/8 (0.32)	
2	3	1/4 (0.64)	
3	5	1/2 (1.27)	
4	2	49/64 (1.96)	TE <sub>11</sub>
5	4	1 (2.54)	TM <sub>01</sub>
6	6	1 17/64 (3.22)	TE <sub>21</sub>
7	7	1 19/32 (4.06)	TM <sub>11</sub>

to 2.27 GHz, the signal at 500 MHz was raised to 568 MHz (2.27 GHz ÷ 4), and the 10 GHz signal was lowered to 9.09 GHz (2.27 GHz x 4) to fit within the instruments' calibrated ranges. Specimen fabrication and testing was initiated on the basis of information in the previous study (with the signal at 10 GHz shifted to 9.5 GHz to accommodate the Narda) before this equipment limitation was fully realized. Consequently, the early tests were performed at the old top frequencies, while later tests were performed at the new frequencies. Although Tables 1 through 6 are arranged logically according to the flaw character of their data, the tests were performed in an experimentally convenient order; consequently, "early tests" refers to the actual test performance order rather than the test series number.

### 3 RESULTS AND ANALYSIS

All results are stated in decibels with respect to free space measurements made without a test panel over the aperture of the shielded enclosure. The electric field vector was propagated perpendicular to the axis of welds and slots in the test panels to achieve the greatest discontinuity in the current flow in the test panels. This was expected to cause slots to be strong re-radiators of signals, thus constituting a worst case of slot axis orientation with respect to electric field vector. For sufficiently small apertures (flaws) the recorded shielding effectiveness was at the top of the receiver's

**Table 7**  
**Equipment Used for Shielding Effectiveness Measurements**

Frequency	Dynamic Range (dB)	Antenna Separation	Equipment Used
10 kHz 40 kHz	116 117	2 ft (.61 m)	Hewlett Packard 202D Signal Generator MB Electronics 2250 Power Amplifier CERL Loop Antenna (radiating) Stoddard NM-12AT Field Intensity Meter Empire LP-105 Loop Antenna (receiving) Singer 500 Shielded Enclosure Leak Detector
200 kHz	108	2 ft (.61 m)	Hewlett Packard 606 Signal Generator Electronic Navigation Industries 310L Amplifier CERL Matched Loop Antenna (radiating) Stoddard NM-12AT Field Intensity Meter Empire LM-105 Loop Antenna (receiving)
1 MHz 30 MHz	104 103	2 ft (.61 m)	Hewlett Packard 606 Signal Generator Electronic Navigation Industries 310L Amplifier CERL Matched Loop Antennas (radiating) Empire NF105 Field Intensity Meter, TA Tuning Head Empire LP-105 Loop Antenna (receiving) Hewlett Packard 355D Attenuator Hewlett Packard 355C Attenuator
500 MHz 568 MHz	103 103	2m	Maxson 1141A Power Oscillator CERL Dipole Antenna (radiating) Empire NF105 Field Intensity Meter, T-3 Tuning Head Empire DM-105 T3 Dipole Antenna (receiving)
2.27 GHz 2.5 GHz	121 144	18 in. (.46 m)	Maxson 1141A Power Oscillator S-Band Waveguide (radiating) Polarad RS-T Receiver S-Band Horn PRD Electronics 1211 Isolator
9.09 GHz 9.5 GHz	115 111	12 in. (.30 m)	Narda 18500B RF Power Pulser X-Band Waveguide (radiating) Polarad RX-T Receiver X-Band Horn (receiving)

dynamic range. Consequently, the actual shielding effectiveness of the flaw may have been greater than recorded. The dynamic range of instrumentation and specified minimum shielding effectiveness are shown as functions of frequency in Figure 10. (The dynamic range is also the shielding effectiveness at zero flaw size, shown in the remaining figures.) The dynamic range was at least 24 dB above the specified minimum shielding effectiveness.

Shielding effectiveness data for a sound weld are also shown in Figure 10. These data are below the dynamic range only at the extreme frequencies, 10 kHz and 9 GHz, and are always over 100 dB shielding effectiveness. Carlson's data<sup>6</sup> for a sound weld are also shown in the figure. Those data are at the dynamic range stated in the Carlson report for almost all the test frequencies. Moreover, those data are in general higher than the data obtained in this study, due to the greater dynamic range obtained in Carlson's work. Why the ranges differ is uncertain.

The data for each test series are divided into two groups by frequency to simplify graphing. Figures 11 and 12 present shielding data for butted plates. The data are somewhat paired: 10 and 40 kHz, 200 kHz and 1 MHz, 30 and 500 MHz, and 2.5 and 9.5 GHz. The data as functions of frequency are generally not monotonic, but have many extrema. Table 1 and Figure 12 show that none of the calculated resonances and anti-resonances were observed. The data for 200 kHz and higher frequencies are virtually constant for slot lengths less than about 3.5 in. (8.89 cm), indicating that the actual shielding effectivenesses of such small flaws exceeded the instrumentation's dynamic range. Three transition flaw sizes can be determined for the three minimum specified shielding effectiveness levels and associated frequency ranges presented in Figure 10. Table 8 presents these transition flaw sizes and the frequencies at which they were noted.

One may suppose that the more tightly butted plates will have better conductivity and permeability across the slot width than those that are less tightly butted. This tightness was an uncontrolled fabrication factor, which may account for some of the extrema observed. However, this effect can be considered influential only when *all* the shielding data at a given slot length rise or fall sharply, reflecting a respective

tightness or looseness of the joint relative to that of adjacent slot lengths. This is based on the observation that a tightly butted slot will shield better than a loosely butted one, regardless of the frequency. The frequency-independent drop in shielding effectiveness at a slot length of 4.7 in. (11.94 cm) observed in Figures 11 and 12 may be due to the joint tightness factor.

Also shown in Figures 11 and 12 are Carlson's data on gapless, unwelded segments of 1-, 4-, and 12-in. (1.27-, 10.16-, and 30.48 cm) lengths, his specimens P-1, P-2, and P-3, respectively. Those data are well imbedded in the data obtained in this study and are somewhat similarly paired by frequency. Agreement between the two sets of data is tolerable at 10 kHz, 200 kHz, and 1 MHz, but is generally not good at other frequencies.

Figures 13 and 14 present shielding data for slotted plates. The data in Figure 13 show a strong trend of decreasing shielding effectiveness with increasing slot length. The data are very closely grouped, indicating a distinct insensitivity of shielding to frequency. The data of 30 and 568 MHz generally run with the lower frequency data. However, the data at 2.27 and 9.09 GHz form a band separate from the other data. First-order resonances at 9.09 and 2.27 GHz were observed at the calculated resonant slot lengths of ~0.6 in. (1.52 cm) and ~2.6 in. (5.16 cm), respectively, as evidenced by the sharp drops in shielding effectiveness at those slot length-frequency combinations (Table 2 and Figure 14). The slight dip at 10.4 in. (26.42 cm) and 568 MHz may also be due to a first-order resonance. No second-order resonances or anti-resonances were observed. None of the data in Figures 13 and 14 exceeded the dynamic range. The three transition flaw sizes are reported in Table 8. The effect of slots in the GHz range has been discussed by Jarva.<sup>7</sup>

Data for the Carlson specimen P-4 with a slot 1 in. (2.54 cm) long by 0.06 in. (1.5 cm) wide are also reported in Figures 13 and 14. These data agree with the data obtained in this study except at the two highest frequencies. Since 1 in. (2.54 cm) is not a first-order resonance for either 2.5 or 10 GHz, the shielding data from Carlson's specimen should be better than the near-resonant data at 2.27 and 9.09 GHz.

<sup>6</sup>K. W. Carlson, *The Effect of Weld Defects on RFI Shielding Effectiveness*, Technical Report M-43/AD773716 (CERL, January 1974).

<sup>7</sup>W. Jarva, "Shielding Tests for Cables and Small Enclosures in the 1- to 10-GHz Range," *IEEE Trans. Electromagnetic Compatibility*, Vol 12, No. 1 (1970), pp 12-24.

**Table 8**  
**Transition Flaw Sizes for Various Test Geometries**

Flaw Type	Transition Flaw Size by Shielding Level		
	70 dB ( $\leq$ 200 kHz)	80 dB (200 kHz $<$ 3 GHz)	60 dB ( $\geq$ 3 GHz)
Butted Plate	4.7 in. ( $\omega$ 10 kHz) (11.94 cm)	9.4 in. ( $\omega$ 1 MHz) (23.88 cm)	4.7 in. ( $\omega$ $\sim$ 9 GHz) (11.94 cm)
Slotted Plate	1.9 in. ( $\omega$ 10 kHz) (4.83 cm)	0.6 in. ( $\omega$ $\sim$ 2 GHz) (1.52 cm)	0.3 in. ( $\omega$ $\sim$ 9 GHz) (0.76 cm)
Wide-Slot Plate	1.3 in. ( $\omega$ 10 kHz) (3.30 cm)	0.4 in. ( $\omega$ $\sim$ 2 GHz) (1.02 cm)	0.4 in. ( $\omega$ $\sim$ 9 GHz) (1.02 cm)
Backing-Strip Plate	4.7 in. ( $\omega$ 10 kHz) (11.94 cm)	4.4 in. ( $\omega$ $\sim$ 2 GHz) (11.18 cm)	4.7 in. ( $\omega$ $\sim$ 9 GHz) (11.94 cm)
Slotted Backing-Strip Plate	2 in. ( $\omega$ 40 kHz) (5.08 cm)	0.3 in. ( $\omega$ 1 MHz & 2 GHz) (0.76 cm)	0.3 in. ( $\omega$ $\sim$ 9 GHz) (0.76 cm)
Drilled Plate	1 in. ( $\omega$ 10 kHz) (2.54 cm)	0.3 in. ( $\omega$ $\sim$ 2 GHz) (0.76 cm)	0.3 in. ( $\omega$ $\sim$ 9 GHz) (0.76 cm)

Shielding data for wide-slot plates are shown in Figures 15 and 16. The three lowest frequencies in Figure 15 form a very narrow band; the fourth fits well among them except at one point. In Figure 16, the data fall into two bands by frequency. Using Table 3 with Figure 16 shows that the data for 2.27 and 9.09 GHz fall rapidly until their first resonant slot lengths are reached. Thereafter, the data vary little. Data at lower frequencies display the expected decrease in shielding with increasing slot length. The three transition flaw sizes are recorded in Table 8. No second-order resonances or anti-resonances were observed.

Shielding data for the backing-strip plates are presented in Figures 17 and 18. The data in Figure 17 fall into a band somewhat broader than observed at these frequencies for other test series. Data for 200 kHz and 1 MHz are at the dynamic range for slot lengths up to 3.6 in. (9.14 cm). In Figure 18, the data at 30 and 568 MHz are almost entirely independent of slot length, while the data at 2.27 and 9.09 GHz are grouped into a generally narrow band. Both frequencies in this band drop sharply at a slot length of 0.15 in. (0.38 cm); this is about one-fourth the size calculated for first-order resonance. Since the actual two highest frequencies differed from those for which the resonant slot lengths had been designed, no resonances were observed. The three transition flaw sizes are given in Table 8.

Figures 19 and 20 show the shielding data for the slotted backing-strip plates. The data in Figure 19 form a well-defined band, while the data in Figure 20 form

two bands by frequency. The data at 30 and 568 MHz are at the dynamic range for slot lengths up to 1.2 in. (3.09 cm). The data for the top two frequencies drop quickly with increasing slot lengths, but the slot length at minimum shielding effectiveness does not agree with calculated values. The three transition flaw sizes are shown in Table 8.

Shielding data for drilled plates are presented in Figures 21 and 22. The data in Figure 21 form a single band, while the data in Figure 22 form two bands. The data at 30 and 568 MHz are at the dynamic range for hole diameters up to 1/2 in. (1.27 cm). The data for 2.27 and 9.09 GHz are near the dynamic range for hole diameters up to 1/8 in. (0.32 cm); the data fall as the diameter increases beyond 1/8 in. (0.32 cm). Table 6 and Figure 22 show that the shielding is very low for the first four resonant modes at 9.09 GHz. The effect of holes in the GHz range has also been discussed by Jarva.<sup>8</sup> The three transition flaw sizes are shown in Table 8.

Data from Carlson's "drilled plate" specimen having a 1/16 in. (0.16 cm) diameter hole are given also in Figures 21 and 22. Those data agree fairly well with the data obtained in this study.

Data from Figures 11 through 16 can be compared by progression of defect width. Tightly butted plates

<sup>8</sup>W. Jarva, "Shielding Tests for Cables and Small Enclosures in the 1- to 10-GHz Range," *IEEE Trans. Electromagnetic Compatibility*, Vol 12, No. 1 (1970), pp 12-24.

(Figures 11 and 12) had no detectable resonance; their data generally fell in a broad band. Plates with a narrow discontinuity (Figures 13 and 14) displayed resonances; their data fell into a fairly narrow band. As expected, plates with wide discontinuities (Figures 15 and 16) generally had lower shielding effectiveness at a given slot length than those with narrow slots. However, some wide slots did have greater shielding effectiveness than some narrow slots of the same length.

The effect of a tacked backing strip is mixed. Transition flaw size was not significantly affected below 200 kHz or above 3 GHz. However, use of backing strips halved the transition flaw size in the 200 kHz-3 GHz range (Table 8). The gap between the backing strip and plate may have produced a resonant condition at these intermediate frequencies.

## 4 CONCLUSIONS AND RECOMMENDATIONS

### Conclusions

The data obtained in this study and the Carlson study show that sound welds have a shielding effectiveness far above the minimum specified levels.

Plates having unwelded but tightly butted seams over a moderate length still have very good shielding effectiveness. Lengths up to 4.7 in. (11.94 cm) provided at least 60 dB shielding at all test frequencies. While these defects do allow some radiation to pass, they are incapable of resonant radiation due to the high quality of electrical conductivity afforded by the tight butting. When the seam forms a slot of finite but small width, resonant radiation is observed, and shielding is seriously degraded at key combinations of frequency and slot length. Shielding to 60 dB for slot flaws can be assured only for flaw lengths under 0.3 in. (0.76 cm). Increasing slot width at a fixed slot length and radiation frequency does not necessarily degrade the shielding; it may improve. The general increase in aperture area tends to obscure resonance as slot width increases. Thus, tight cracks or other forms of one-dimensional weld defects will not compromise the shielding effectiveness to less than 60 dB if the defect does not exceed 4½ in. (11.43 cm).

Backing strips placed over seams with unwelded lengths have little effect below 200 kHz and above 3 GHz. Between 200 kHz and 3 GHz, backing strips may halve the tolerable defect length.

Plates having holes as large as 0.3 in. (0.76 cm) can still afford at least 60 dB shielding at all test frequencies. Larger holes can also assure good shielding at selected frequencies. Thus, porosity or other spheroidal weld defects will not compromise shielding effectiveness to less than 60 dB if the defect's major dimension in the plane of the plate does not exceed 0.3 in. (0.76 cm).

No sharp increases in shielding effectiveness were observed at those slot lengths for which anti-resonance was predicted. Consequently, it is doubtful that such a phenomenon occurs. No second-order resonance was observed.

Figures 12 and 18 show that very high shielding effectiveness existed at 300 ~ 500 MHz over a broad range of butted plate defect lengths. The shape of the shielded enclosure used may have permitted the high shielding effectiveness over this frequency range. If so, it may be possible to design a shielded enclosure that offers high shielding effectiveness due to its *geometrical character*. Schulz and his associates<sup>9</sup> have attributed resonance in the 5 to 200 kHz range in typical shielding enclosures to a difference in phase retardation between a path through the shielding material and a path through seams. Schulz also observed that seam effects are negligible below 5 kHz, significant between 50 kHz and 5 MHz, and predominant (along with cavity resonance and material configuration) above 5 MHz.<sup>10</sup>

### Recommendations

Shielding specifications should be changed to incorporate the technical aspects of this report and should permit acceptance of welds that have been visually inspected and found to contain no flaws in excess of the critical flaw sizes. Table 8 can be used to establish inspection and acceptance criteria for SAFEGUARD-type facilities.

The apertures affording tolerable shielding effectiveness were all easily detected visually. Hence, welds need only be visually inspected; radiographic or magnetic particle inspection is not necessary. Porosity that is not open to the surface need not be a concern.

<sup>9</sup>R. B. Schulz, V. C. Plantz, and D. R. Brush, "Low-Frequency Shielding Resonance," *IEEE Trans. Electromagnetic Compatibility*, Vol 10, No. 1 (1968), pp 7-15.

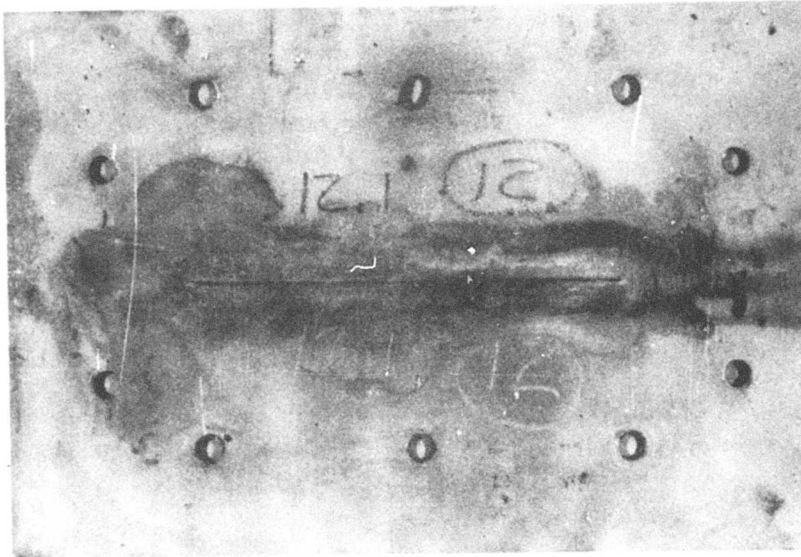
<sup>10</sup>R. B. Schulz, G. C. Huang, and W. L. Williams, "RF Shielding Design," *IEEE Trans. Electromagnetic Compatibility*, Vol 10, No. 1 (1968), pp 168-175.



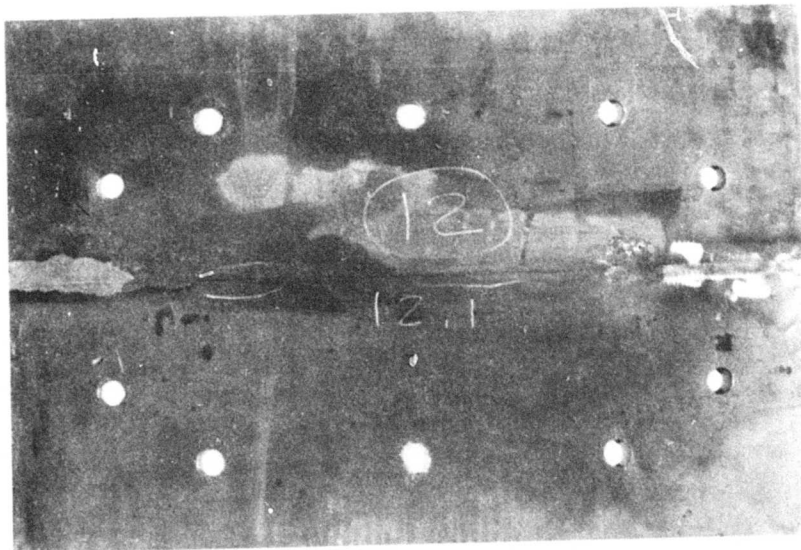
Due to the strong shielding effectiveness encountered in the neighborhood of 500 MHz, effort should be made to develop design principles for shielded enclosure shapes that offer high shielding effectiveness.

## REFERENCES

- Carlson, K. W., *The Effect of Weld Defects on RFI Shielding Effectiveness*, Technical Report M-43/AD773716 (Construction Engineering Research Laboratory [CERL], January 1974).
- Jarva, W., "Shielding Tests for Cables and Small Enclosures in the 1- to 10-GHz Range," *IEEE Trans. Electromagnetic Compatibility*, Vol. 12, No. 1 (1970), pp 12-24.
- Measurement of Shielding Effectiveness of High Performance Shielding Enclosures*, IEEE Standard 299 (Institute of Electrical and Electronic Engineers, 1969).
- Method of Attenuation Measurements for Enclosures, Electromagnetic Shielding, for Electronic Test Purposes*, MIL-STD-285 (Department of Defense, June 1956).
- Schulz, R. B., G. C. Huang, and W. L. Williams, "RF Shielding Design," *IEEE Trans. Electromagnetic Compatibility*, Vol. 10, No. 1 (1968), pp 168-175.
- Schulz, R. B., V. C. Plantz, and D. R. Brush, "Low-Frequency Shielding Resonance," *IEEE Trans. Electromagnetic Compatibility*, Vol. 10, No. 1 (1968), pp 7-15.



a. Shielded enclosure side



b. Transmitter side

Figure 1. Butted plate with 12.1-in. (30.73 cm) slot length.

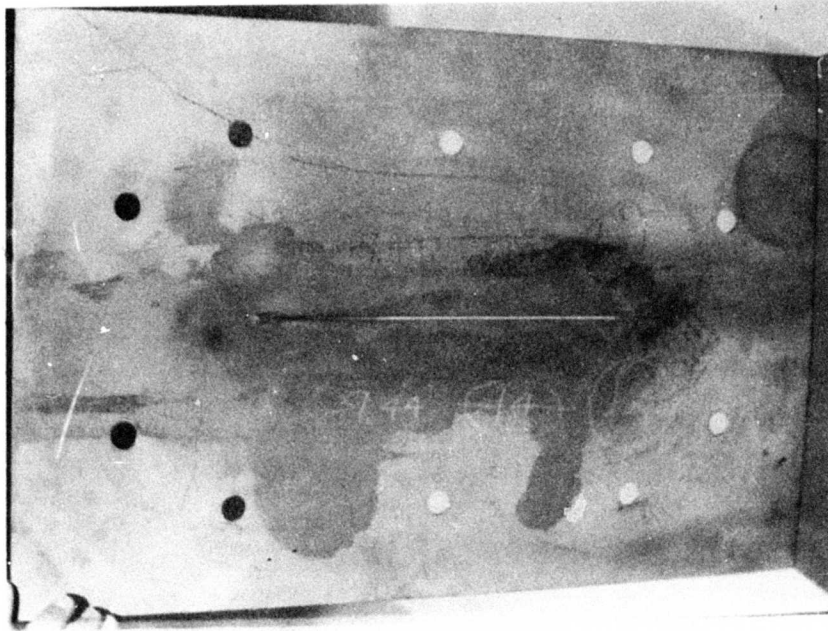


**Figure 2.** Slotted plate with slot 9.44 in. (23.98 cm) long and 1/16 in. (0.16 cm) wide—shielded enclosure side.

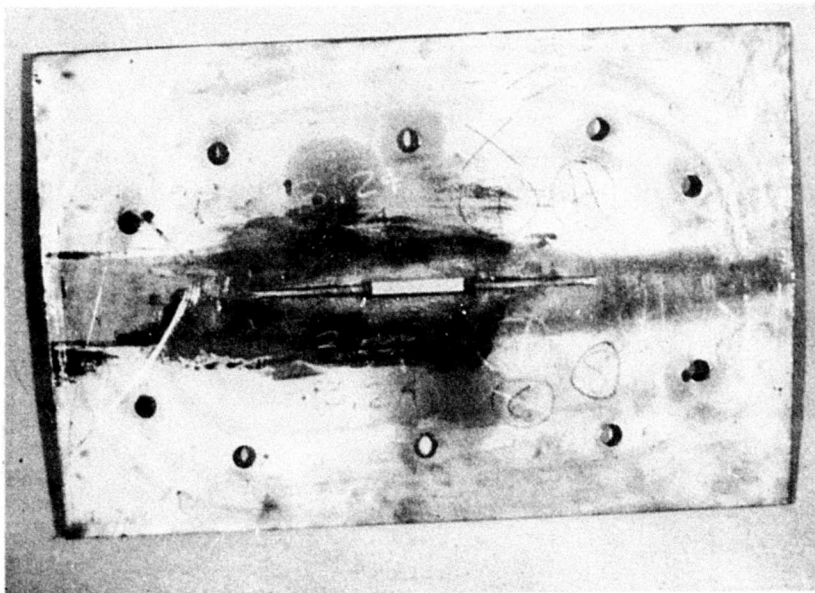
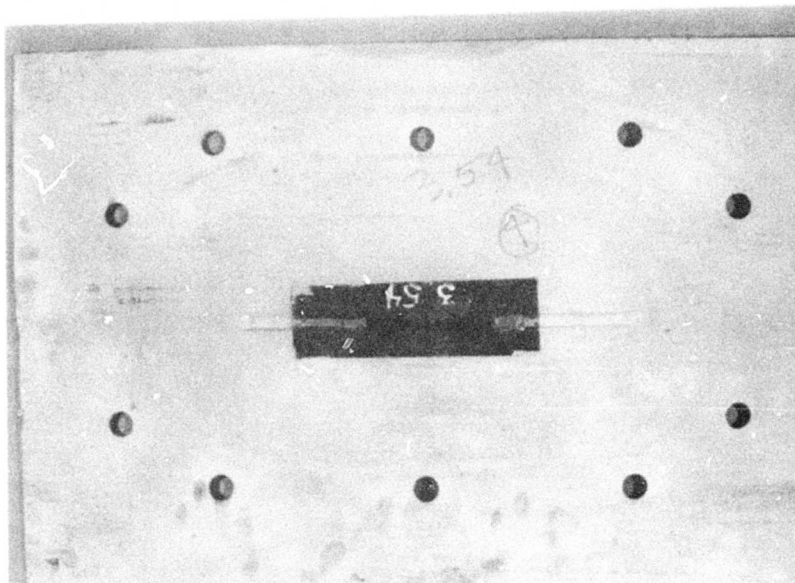
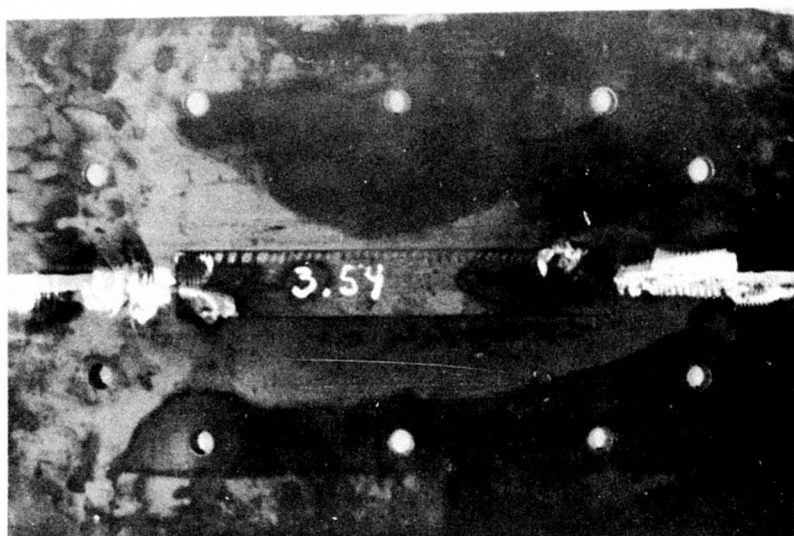


**Figure 3.** Wide-slot plate with slot 3.54 in. (8.99 cm) long and 1/2 in. (1.27 cm) wide—shielded enclosure side.



a. Shielded enclosure side



b. Transmitter side showing tacked backing strip

**Figure 4.** Backing-strip plate with 3.54-in. (8.99 cm) long slot.

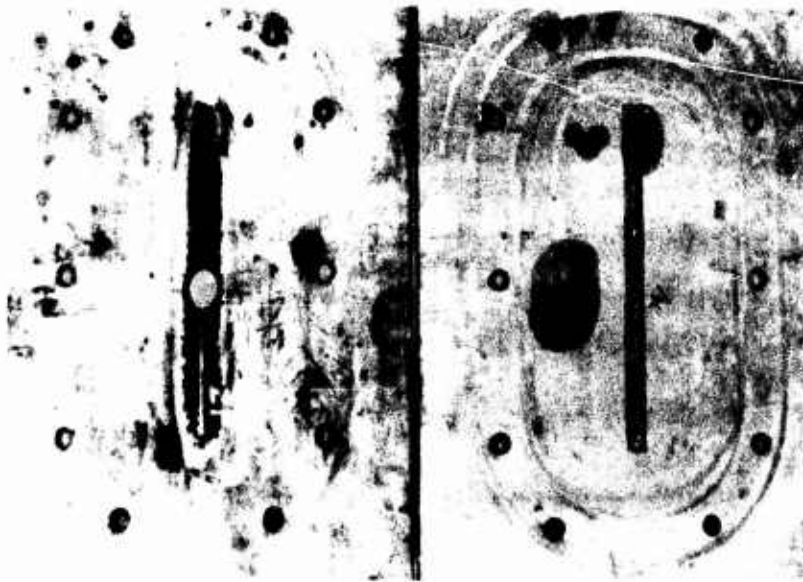


**Figure 5.** Drilled plates shielded enclosure sides. Hole diameters are  $1 \frac{17}{64}$  in. (3.22 cm) (left) and  $\frac{1}{4}$  in. (0.64 cm) (right).

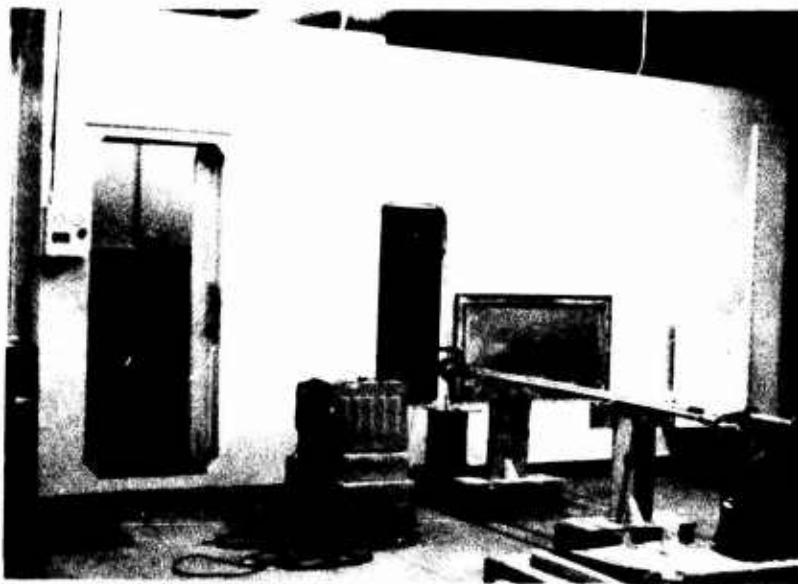


**Figure 6.** Shielded enclosure with cover plate over test panel and door into one of two compartments.

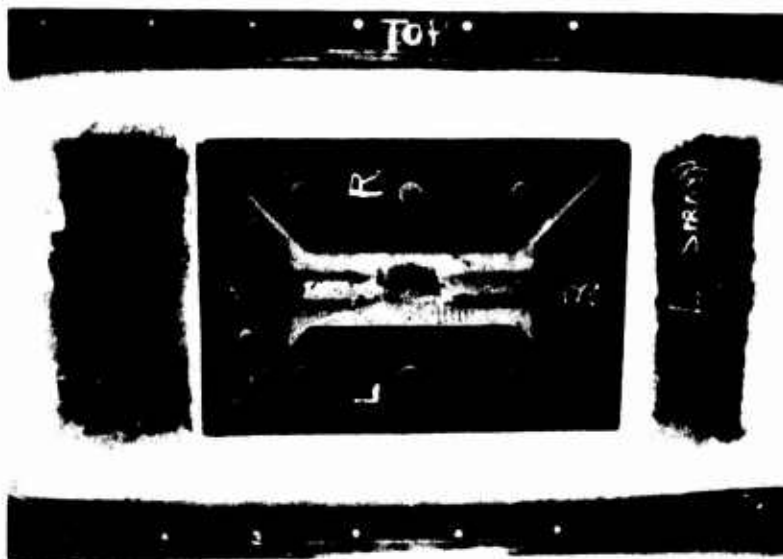


**Figure 7.** Transmitter side of test panel bolted over aperture of shielded enclosure.

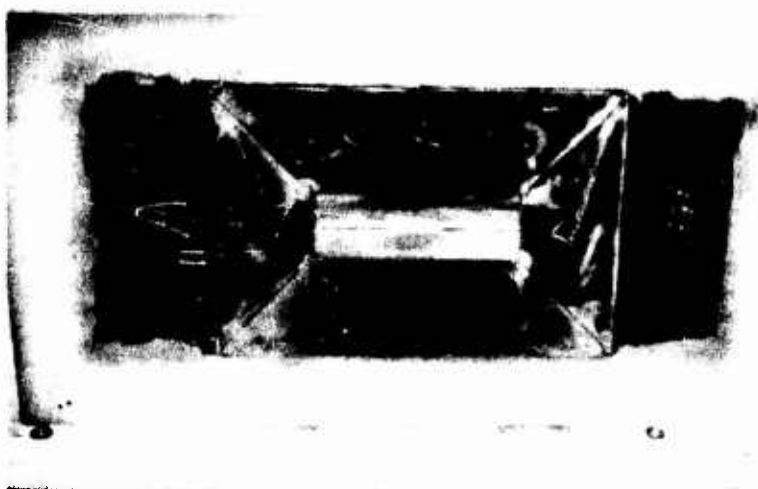


**Figure 8.** View of same panel from within the shielded enclosure.

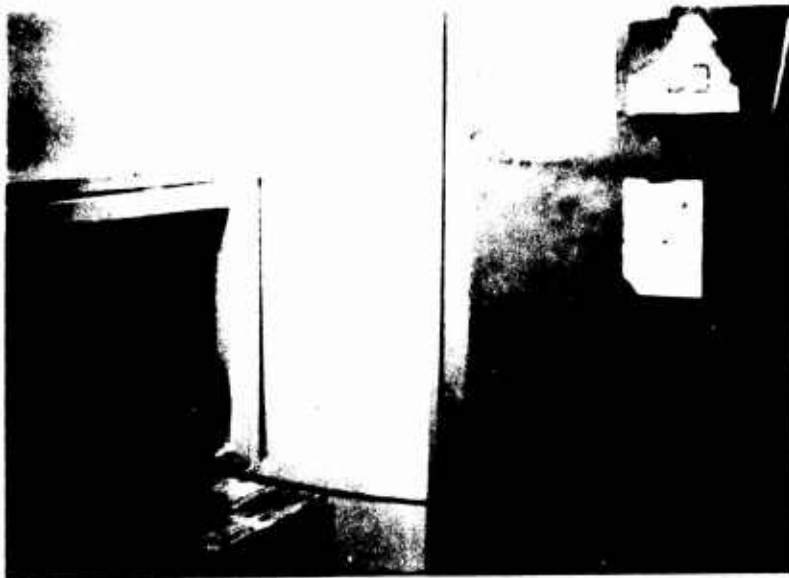


Figure 9. Receiving antenna positioned before test panel. Shielded septum (right) passes antenna cable to receiver in adjacent compartment.

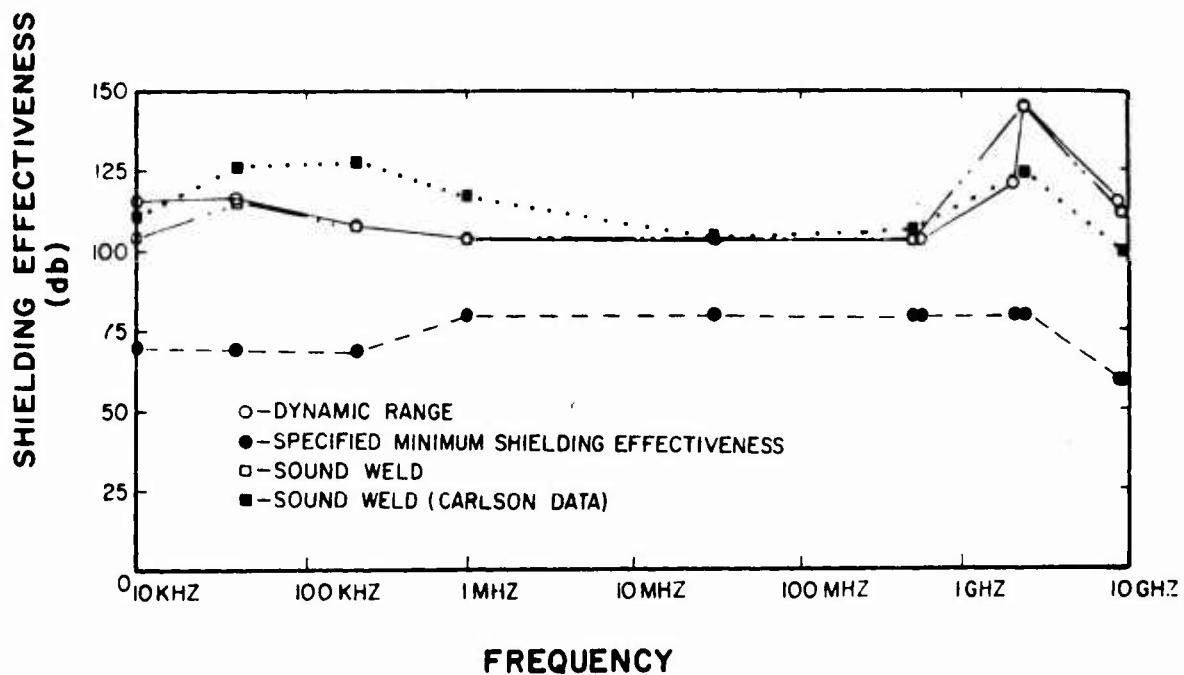


Figure 10. Shielding effectiveness vs frequency.

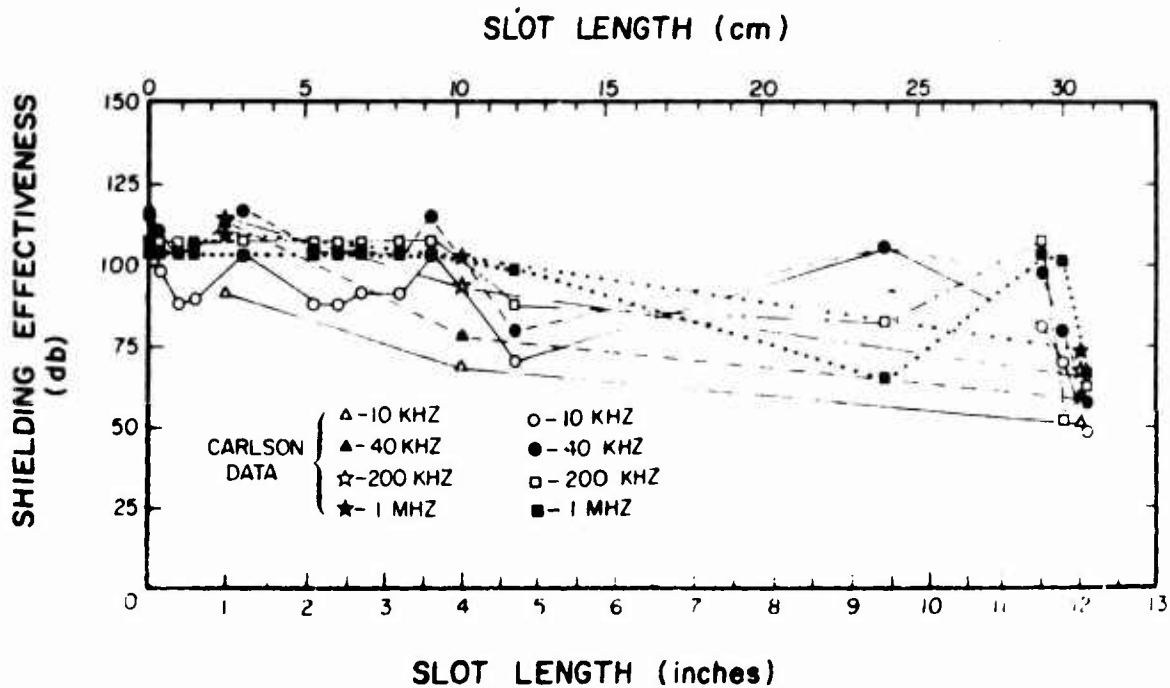


Figure 11. Shielding effectiveness vs slot length for butted plates - 10 kHz to 1 MHz.

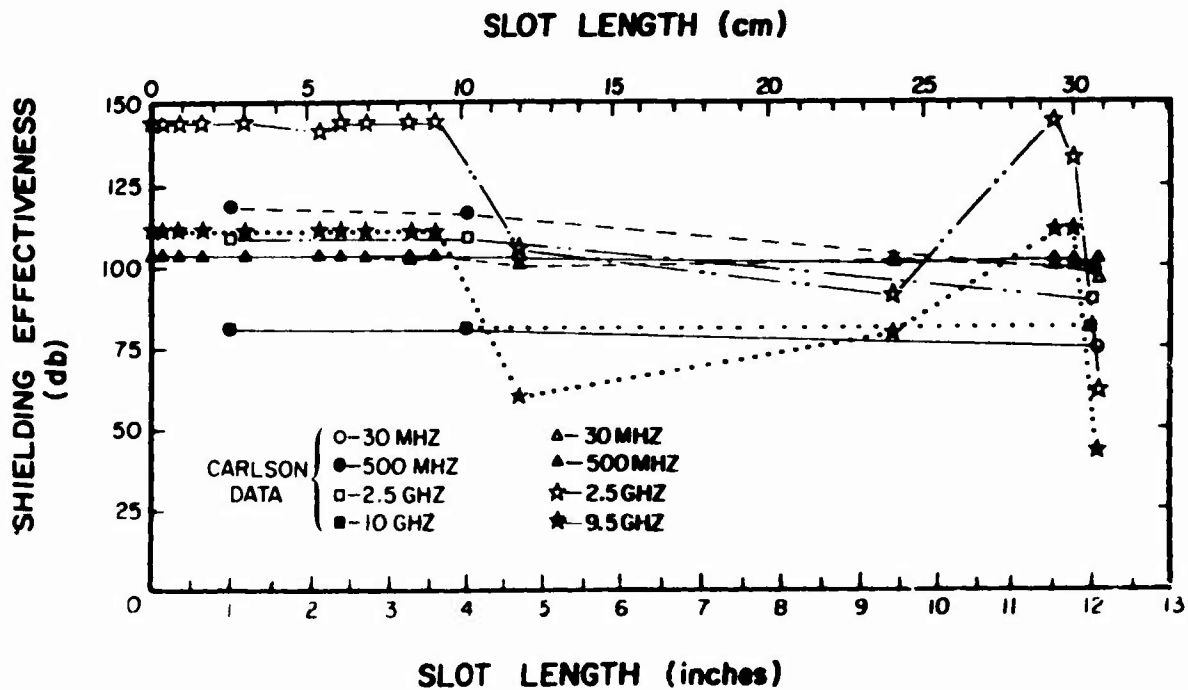


Figure 12. Shielding effectiveness vs slot length for butted plates - 30 MHz to 10 GHz.



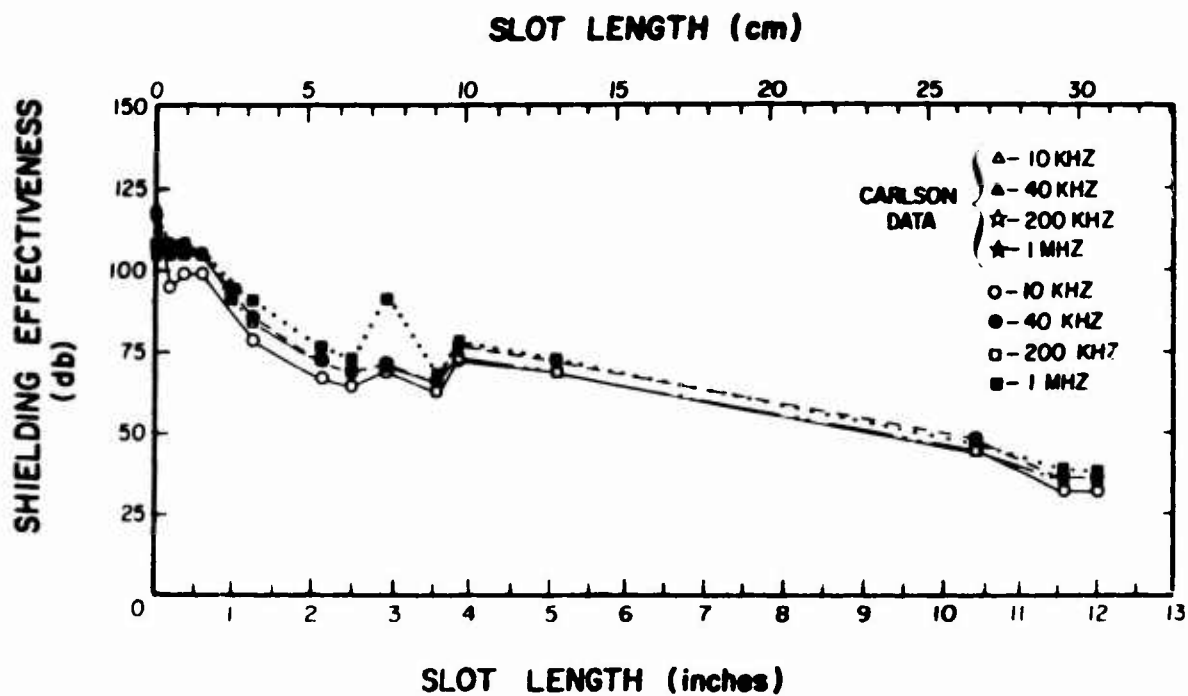


Figure 13. Shielding effectiveness vs slot length for slotted plates 10 kHz to 1 MHz.  
Slot width is 1/16 in. (0.16 cm); Carlson slot width is 0.06 in. (0.15 cm).

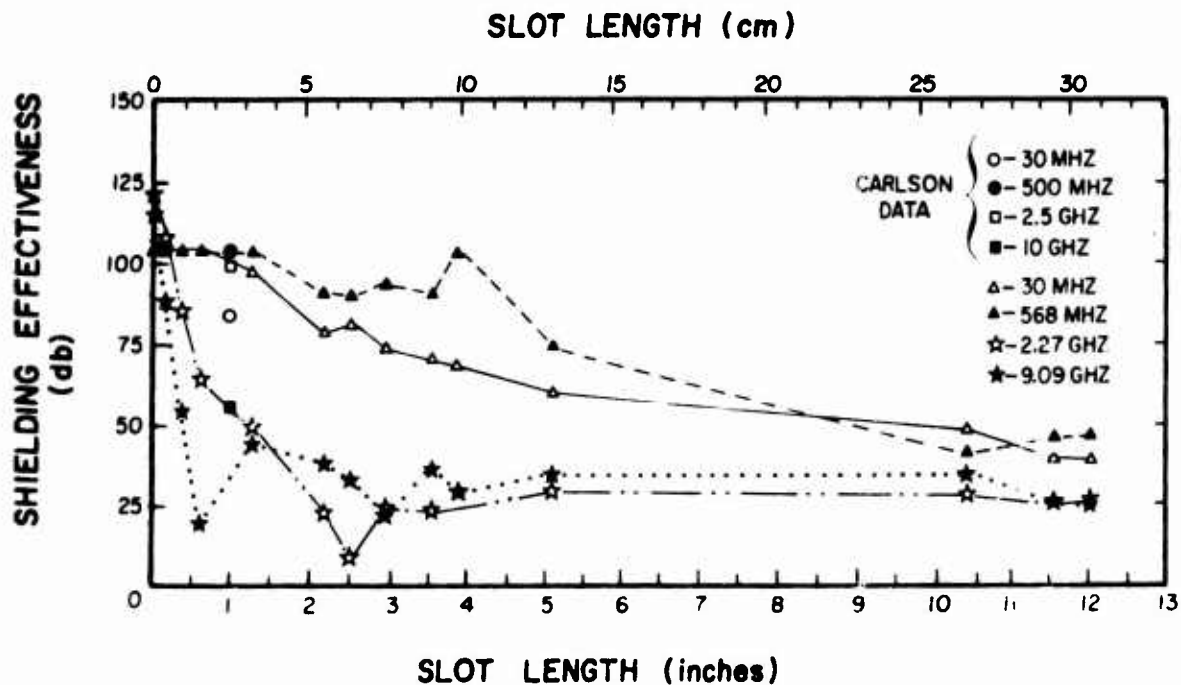


Figure 14. Shielding effectiveness vs slot length for slotted plates—30 MHz to 10 GHz.  
Slot width is 1/16 in. (0.16 cm); Carlson slot width is 0.06 in. (0.15 cm).

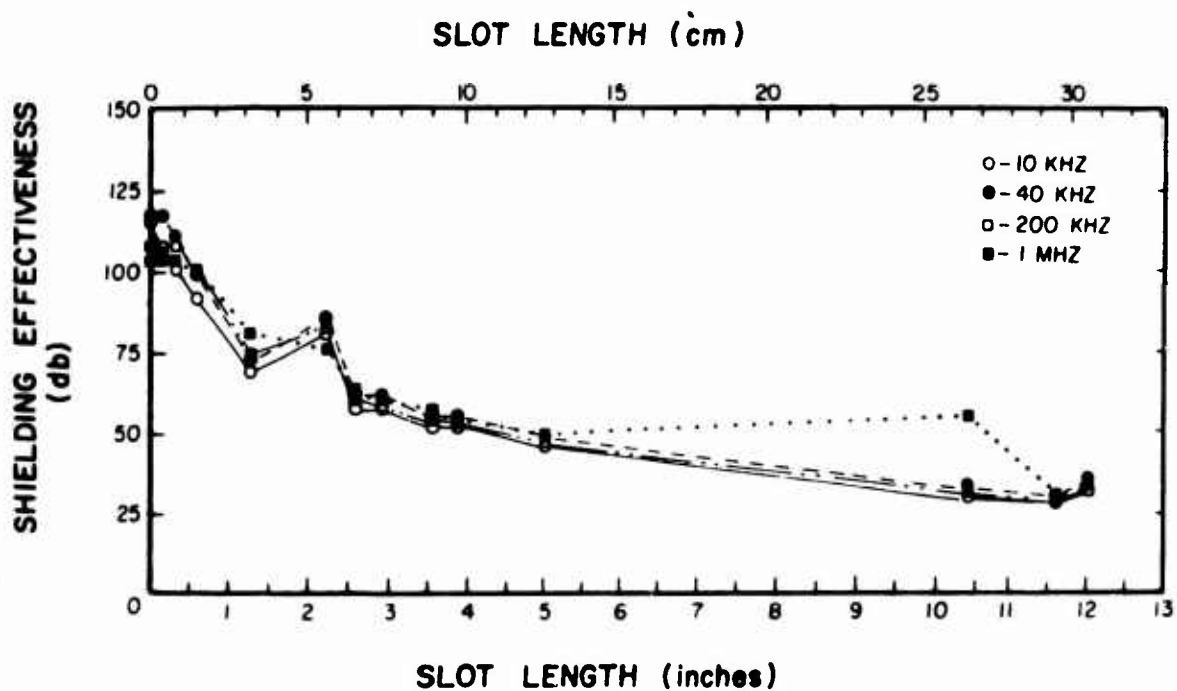


Figure 15. Shielding effectiveness vs slot length for wide-slot plates—10 kHz to 1 MHz. Slot widths are 3/16 in. (0.48 cm) for slot lengths under 1 in. (2.54 cm); other slot widths are 1/2 in. (1.27 cm).

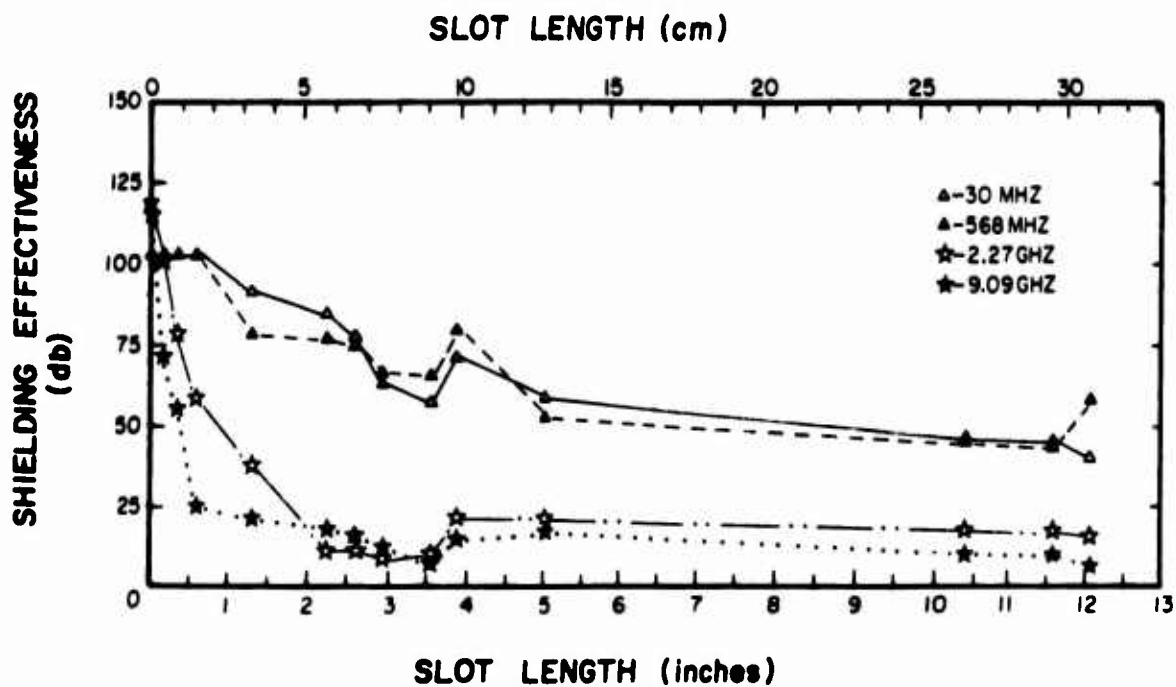


Figure 16. Shielding effectiveness vs slot length for wide-slot plates—30 MHz to 9.09 GHz. Slot widths are 3/16 in. (0.48 cm) for slot lengths under 1 in. (2.54 cm); other slot widths are 1/2 in. (1.27 cm).

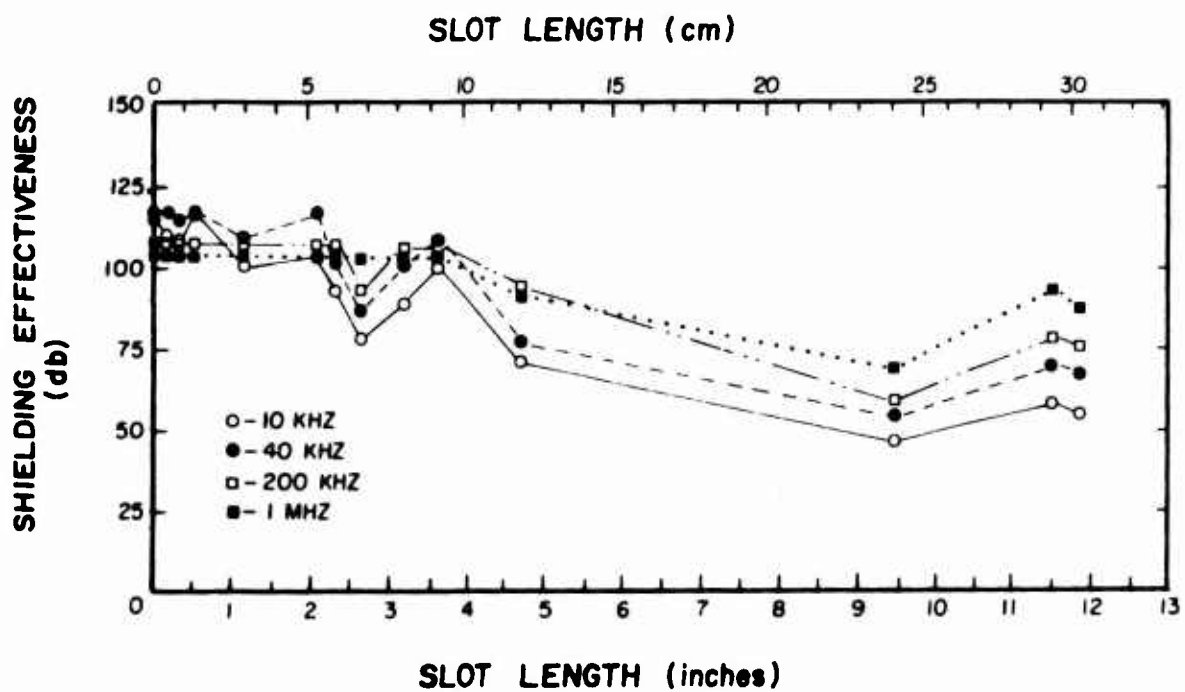


Figure 17. Shielding effectiveness vs slot length for backing-strip plates—10 kHz to 1 MHz.

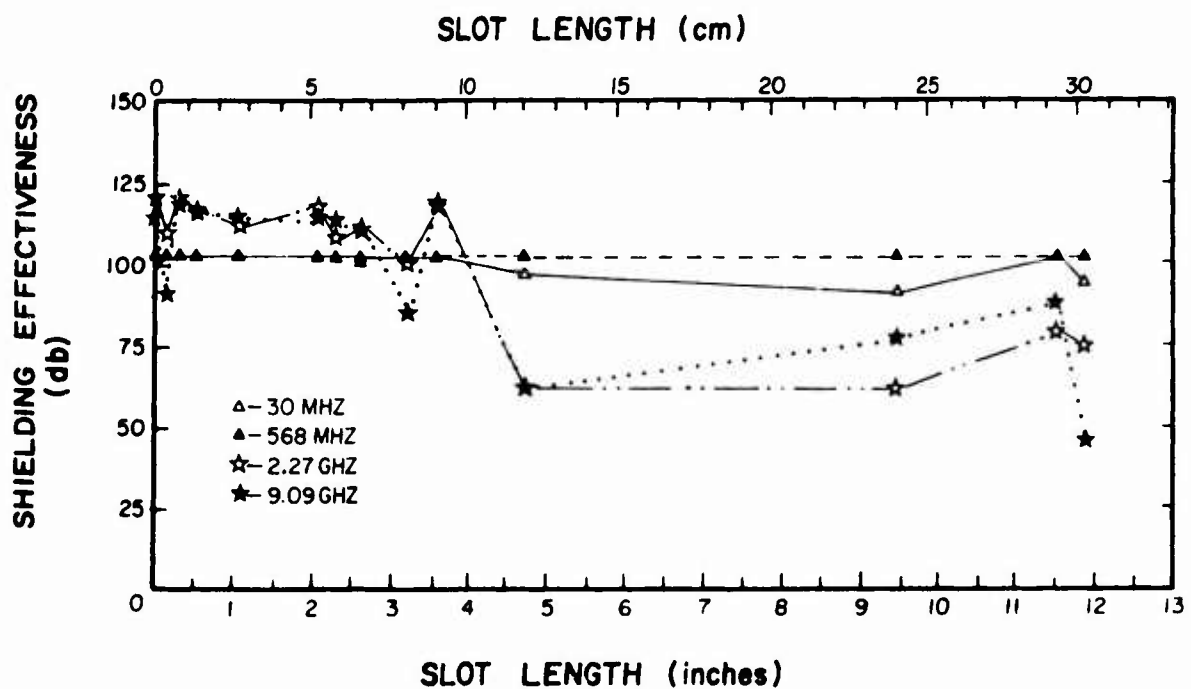


Figure 18. Shielding effectiveness vs slot length for backing-strip plates – 30 MHz to 9.09 GHz.

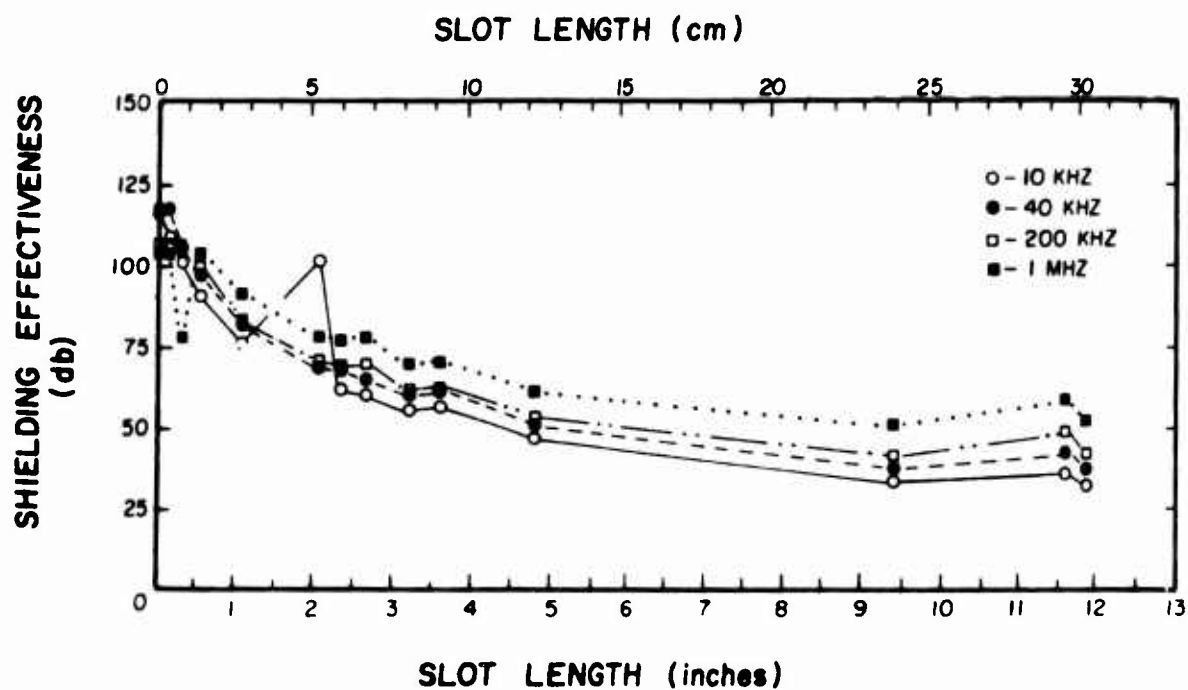


Figure 19. Shielding effectiveness vs slot length for slotted backing-strip plates—10 kHz to 1 MHz. Slots are 1/16 in. (0.16 cm) wide.

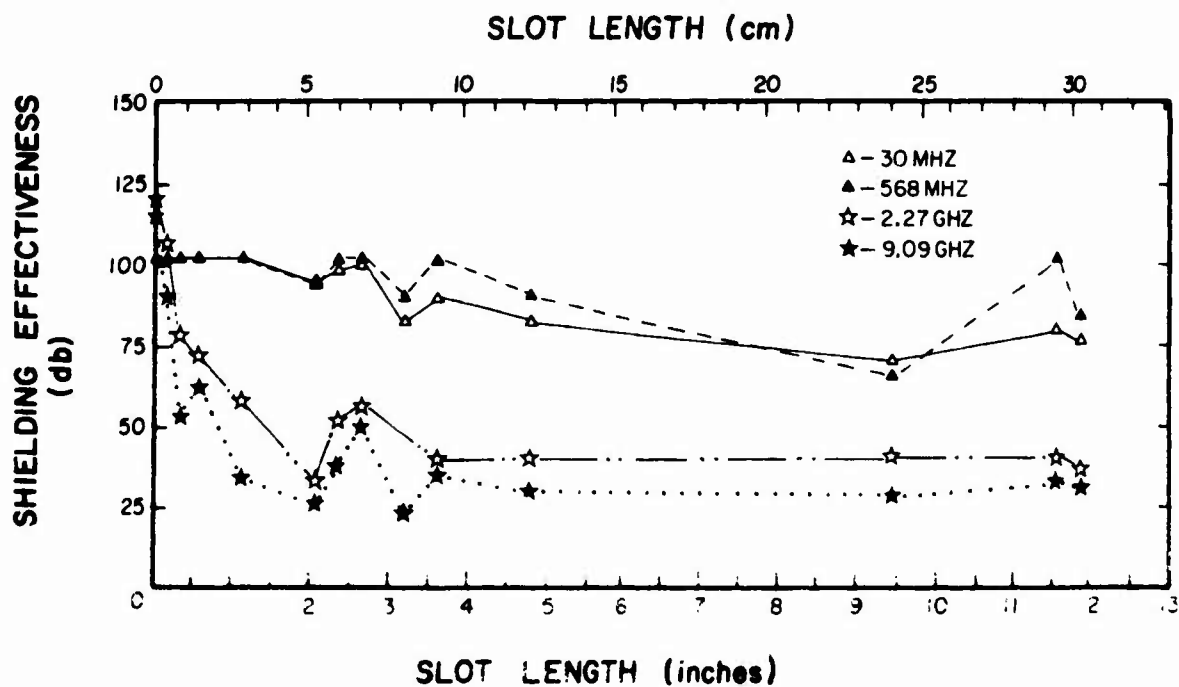


Figure 20. Shielding effectiveness vs slot length for slotted backing-strip plates—30 MHz to 9.09 GHz. Slots are 1/16 in. (0.16 cm) wide.

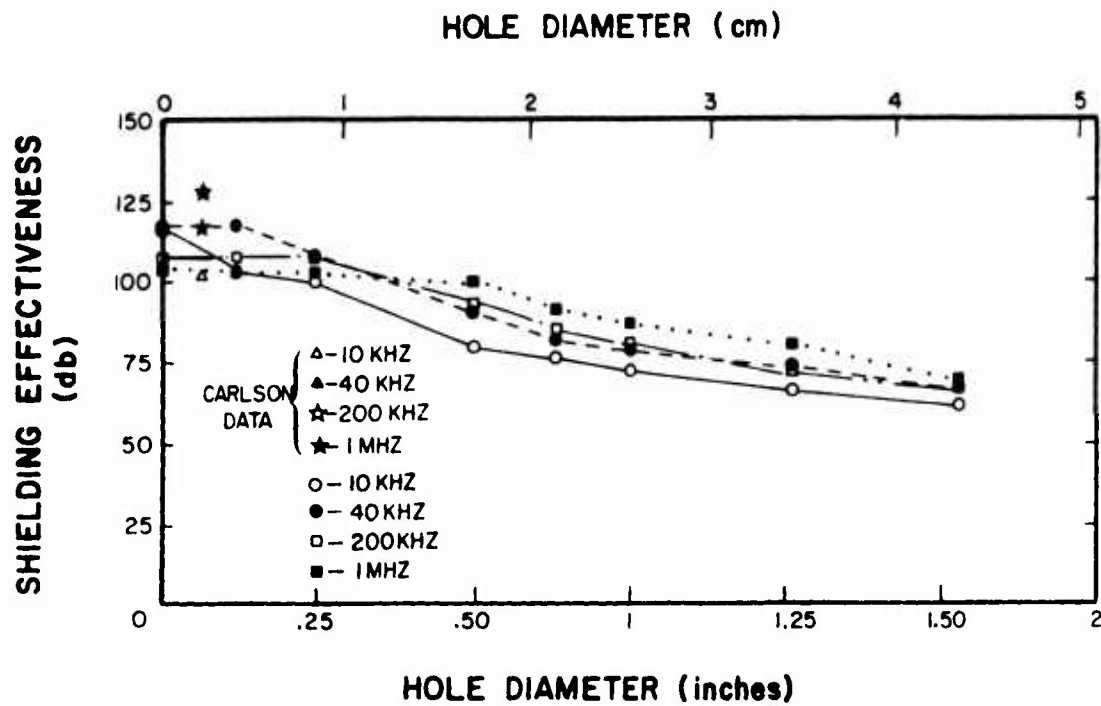


Figure 21. Shielding effectiveness vs hole diameter for drilled plates—10 kHz to 1 MHz.

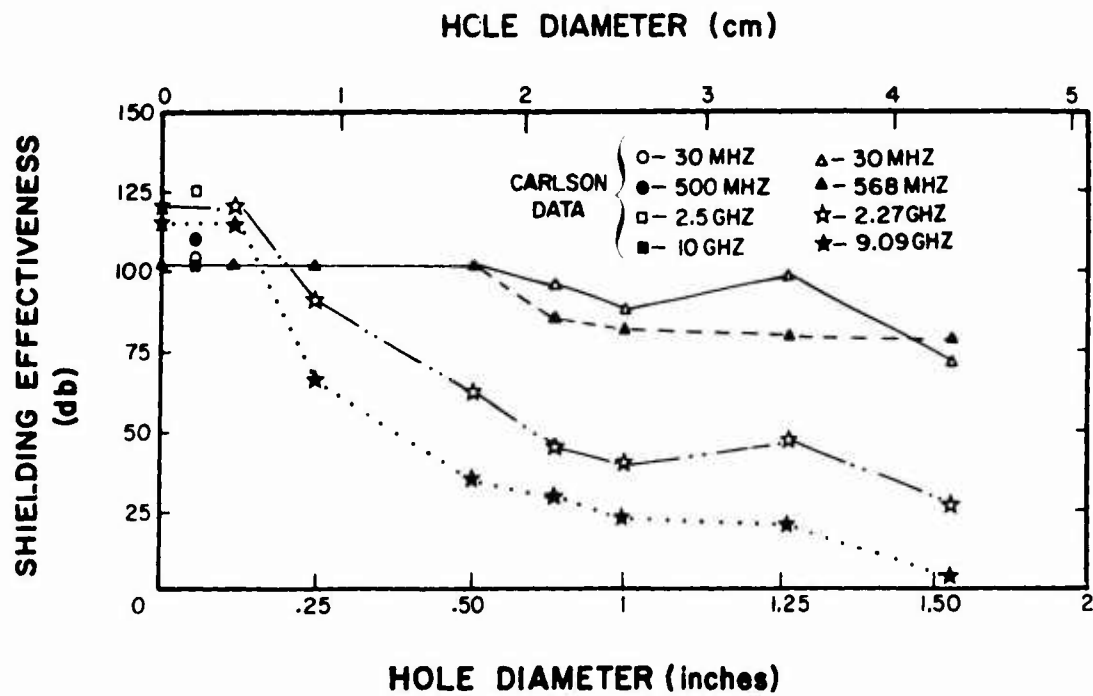


Figure 22. Shielding effectiveness vs hole diameter for drilled plates—30 MHz to 10 GHz.

# CERL DISTRIBUTION

Chief of Engineers  
ATTN: DAEN-MCZ-S (2)  
ATTN: DAEN-ASI-L  
ATTN: DAEN-FLL-A  
ATTN: DAEN-FE  
ATTN: DAEN-RD  
ATTN: DAEN-CHZ-R (3)  
ATTN: DAEN-R (2)  
**ATTN: DAEN-MCD-E**  
Dept of the Army  
WASH DC 20314

U.S. Military Academy  
ATTN: Dept of Mechanics  
ATTN: Library  
West Point, NY 10996

The Engineering School  
Technical Information Br.  
Archives Section (Bldg 270)  
Ft Belvoir, VA 22060

USA Engineering School  
ATTN: ATSEN-DT-LD (2)  
Ft Belvoir, VA 22060

Director  
USA Cold Regions Research  
Engineering Laboratory  
PO Box 282  
Hanover, NH 03755

Director, USA-WES  
ATTN: Concrete Div  
ATTN: Soils Div  
ATTN: Library  
PO Box 631  
Vicksburg, MS 39181

Deputy Chief of Staff  
for Logistics  
US Army, The Pentagon  
WASH DC 20310

The Army Library  
Office of the Adjutant  
General  
Room 1A530, The Pentagon  
WASH DC 20315

HQDA (SGRD/Chief),  
Sanitary Engr Br  
WASH DC 20314

Dept of the Army  
ATTN: EACICT-P  
HQ I Corps (Group)  
APO San Francisco 96358

Commander-in-Chief  
US Army, Europe  
ATTN: AEAEN  
APO New York, NY 09403

Commander, Naval Facilities  
Engineering Command  
ATTN: Dep Ass't Commander  
for Design & Spec (04D)  
200 Stovall Street  
Alexandria, VA 22332

Chief, Naval Operations  
ATTN: The Library  
Dept of the Navy  
WASH DC 20360

Chief, Hydrographic Office  
ATTN: The Library  
Dept of the Navy  
WASH DC 20360

Chief  
Naval Air Systems Command  
ATTN: The Library  
Dept of the Navy  
WASH DC 20360

Naval Civil Engineering Lab  
Technical Library Code L31  
Port Hueneme, CA 93043

Officer in Charge  
Naval Civil Engineering Lab  
Port Hueneme, CA 93043

AF Civil Engr Center/PG  
Tyndall AFB, FL 32401

AFWL/Civil Engr Div  
Kirtland AFB, NM 87117

AF/PREE  
Bolling AFB, DC 20332

AF/RDPQ  
WASH DC 20330

Each Division Engineer  
US Army Engr Div  
ATTN: Library  
ATTN: Chief, Engr Div

Each District Engineer  
US Army Engr District  
ATTN: Library  
ATTN: Chief, Engr Div

Defense Documentation  
Center  
ATTN: TCA (12)  
Cameron Station  
Alexandria, VA 22314

Chief, Airports Standard  
Div-AS58  
Federal Aviation Administration  
800 Independence Ave SW  
WASH DC 20553

Office of Management Svc,  
MS 110 - FAA  
800 Independence Ave SW  
WASH DC 20553

Transportation Research Board  
National Research Council (3)  
2101 Constitution Ave  
WASH DC 20418

Dept of Trans Library  
Acquisitions Section (SR)  
TAD-491.1  
400 7th Street SW  
WASH DC 20590

Engineering Societies Library  
345 East 47th Street  
New York, NY 10017

Library of Congress  
Exchange and Gift Div.  
ATTN: American & British  
WASH DC 20540

Superintendent of Documents  
Div of Public Documents  
ATTN: Library (2)  
US Govt Printing Office  
WASH DC 20402

Commanding General  
USA Engr Command, Europe  
APO New York, NY 09405

Engineer  
US Army, Alaska  
APO Seattle, WA 98242

Commander, TRADOC  
Office of the Engineer  
ATTN: ATEN  
Ft Monroe, VA 23651

Bldg Research Advisory Board  
National Academy of Sciences  
2101 Constitution Avenue  
WASH DC 20418

Air Force Weapons Lab  
Technical Library (DOUL)  
Kirtland AFB, NM 87117

Commanding General  
US Army Forces Command  
ATTN: AFEN-FEB  
Ft. McPherson, GA 30330

Commanding General, 5th USA  
ATTN: Engineer  
Ft Sam Houston, TX 78234

Commanding General, 6th USA  
ATTN: Engineer  
Presidio of San Francisco, CA  
94129

Plastics Technical Evaluation  
Center  
ATTN: SMUPA-VP3  
Picatinny Arsenal  
Dover, NY 07801

Institute of Defense Analysis  
400 Army-Navy Drive  
Arlington, VA 22202

Defense Logistics Studies Infor-  
mation Exchange (2)  
U.S. Army Logistics Management  
Center  
ATTN: AMAMC-D  
Ft. Lee, VA 23801

Chief, Civil Engineering Research  
Division  
Air Force Weapons Lab, AFW  
Kirtland AFB, NM 87117

Coastal Engineering  
Research Center  
Kingman Bldg  
ATTN: Library  
Ft. Belvoir, VA 22060

Dept of the Army  
HQ 15th Engineer Battalion  
9th Infantry Division  
Ft. Lewis, WA 98433

Main Library, Documents  
Section  
State University of  
New York at Stony Brook  
Stony Brook, NY 11790

W. N. Lofroos, P.E.  
Chief, Bureau of Planning  
Dept of Transportation  
605 Suwannee St.  
Tallahassee, FL 32304

Dept of the Army  
U.S. Army Human Engr Lab  
ATTN: AMZHE/J. D. Weisz  
Aberdeen Proving Ground,  
MD 21005

Naval Facilities Engineering  
Command  
ATTN: Code 04  
200 Stovall St.  
Alexandria, VA 22332

Ass't Chief of Engineers  
ATTN: DAEN-ZCI  
WASH DC 20314

314/DEEE  
Little Rock Air Force Base  
Jacksonville, AR 72076

Defense Nuclear Agency  
ATTN: DNA-SPSS  
WASH DC 20305

Chief of Engineers  
ATTN: DAEN-IM: 12)  
Dept of the Army  
WASH DC 20314

For forwarding to:

British Liaison Officer (5)  
U. S. Army Mobility Equipment  
Research and Development Center  
Fort Belvoir, VA 22060

Canadian Forces Liaison Officer (4)  
U. S. Army Mobility Equipment  
Research and Development Center  
Fort Belvoir, VA 22060

Chief  
Construction Engineer  
Air Service Branch  
Department of Transport  
Ottawa, Ontario, Canada

Div of Bldg Research  
National Research Council  
Montreal Road  
Ottawa, Ontario, K1A0R6

National Defense Headquarters  
Director General of Construction  
Ottawa, Ontario K1A 0K2  
Canada